Z-A Dependence of Coherent Muon to Electron Conversion

arXiv 2401.15025

Léo Borrel, David Hitlin, Sophie Middleton

California Institute of Technology, Pasadena, CA

September 19, 2024

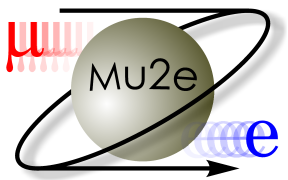

Caltech

Goal

Improve the calculation of the coherent muon to electron conversion rate for a wide range of isotopes

1. Add muonic X-ray experimental data to electron scattering dataset
2. Include the effect of nuclear quadrupole deformation
3. Account for the difference between neutron and proton distribution
4. Present an alternative normalization for the muon conversion rate

R. Kitano *et al.*, Phys. Rev. D **66**, 096002 (2002)
V. Cirigliano *et al.*, Phys. Rev. D **80**, 013002 (2009)
J. Heeck *et al.*, Nucl. Phys. B **980**, 115833 (2022)

Theoretical background

Most general Lepton Flavor Violation interaction Lagrangian):

$$\mathcal{L} = -\frac{4G_F}{\sqrt{2}}\left(m_\mu A_R \bar{\mu}\sigma^{\mu\nu}P_L e F_{\mu\nu} + m_\mu A_L \bar{\mu}\sigma^{\mu\nu}P_R e F_{\mu\nu} + h.c.\right) \quad \text{[Dipole]}$$

$$- \frac{G_F}{\sqrt{2}} \sum_{q=u,d,s} \Big[\left(g_{LS(q)}\bar{e}P_R\mu + g_{RS(q)}\bar{e}P_L\mu\right)\bar{q}q \quad \text{[Scalar]}$$

$$+ \left(g_{LP(q)}\bar{e}P_R\mu + g_{RP(q)}\bar{e}P_L\mu\right)\bar{q}\gamma_5 q \quad \text{[Pseudo-scalar]}$$

$$+ \left(g_{LV(q)}\bar{e}\gamma^\mu P_L\mu + g_{RV(q)}\bar{e}\gamma^\mu P_R\mu\right)\bar{q}\gamma_\mu q \quad \text{[Vector]}$$

$$+ \left(g_{LA(q)}\bar{e}\gamma^\mu P_L\mu + g_{RA(q)}\bar{e}\gamma^\mu P_R\mu\right)\bar{q}\gamma_\mu\gamma_5 q \quad \text{[Axial]}$$

$$+ \frac{1}{2}\left(g_{LT(q)}\bar{e}\sigma^{\mu\nu}P_R\mu + g_{RT(q)}\bar{e}\sigma^{\mu\nu}P_L\mu\right)\bar{q}\sigma_{\mu\nu}q + h.c.\Big] \quad \text{[Tensor]}$$

R. Kitano *et al.*, Phys. Rev. D **66**, 096002 (2002)

Equations

conversion rate:

$$\omega_{conv} = 2G_f^2 \left| A_R^* D + \tilde{g}_{LS}^{(p)} S^{(p)} + \tilde{g}_{LS}^{(n)} S^{(n)} + \tilde{g}_{LV}^{(p)} V^{(p)} + \tilde{g}_{LV}^{(n)} S^{(n)} \right|^2$$
$$+ 2G_f^2 \left| A_L^* D + \tilde{g}_{RS}^{(p)} S^{(p)} + \tilde{g}_{RS}^{(n)} S^{(n)} + \tilde{g}_{RV}^{(p)} V^{(p)} + \tilde{g}_{RV}^{(n)} S^{(n)} \right|^2$$

Overlap integrals:

$$D = \frac{4}{\sqrt{2}} m_\mu \int_0^\infty [-E(r)] \left(g_e^- f_\mu^- + f_e^- g_\mu^- \right) r^2 dr$$
$$S^{(p)} = \frac{1}{2\sqrt{2}} \int_0^\infty Z\rho^{(p)}(r) \left(g_e^- g_\mu^- - f_e^- f_\mu^- \right) r^2 dr$$
$$S^{(n)} = \frac{1}{2\sqrt{2}} \int_0^\infty (A-Z)\rho^{(n)}(r) \left(g_e^- g_\mu^- - f_e^- f_\mu^- \right) r^2 dr$$
$$V^{(p)} = \frac{1}{2\sqrt{2}} \int_0^\infty Z\rho^{(p)}(r) \left(g_e^- g_\mu^- + f_e^- f_\mu^- \right) r^2 dr$$
$$V^{(n)} = \frac{1}{2\sqrt{2}} \int_0^\infty (A-Z)\rho^{(n)}(r) \left(g_e^- g_\mu^- + f_e^- f_\mu^- \right) r^2 dr$$

Previous work

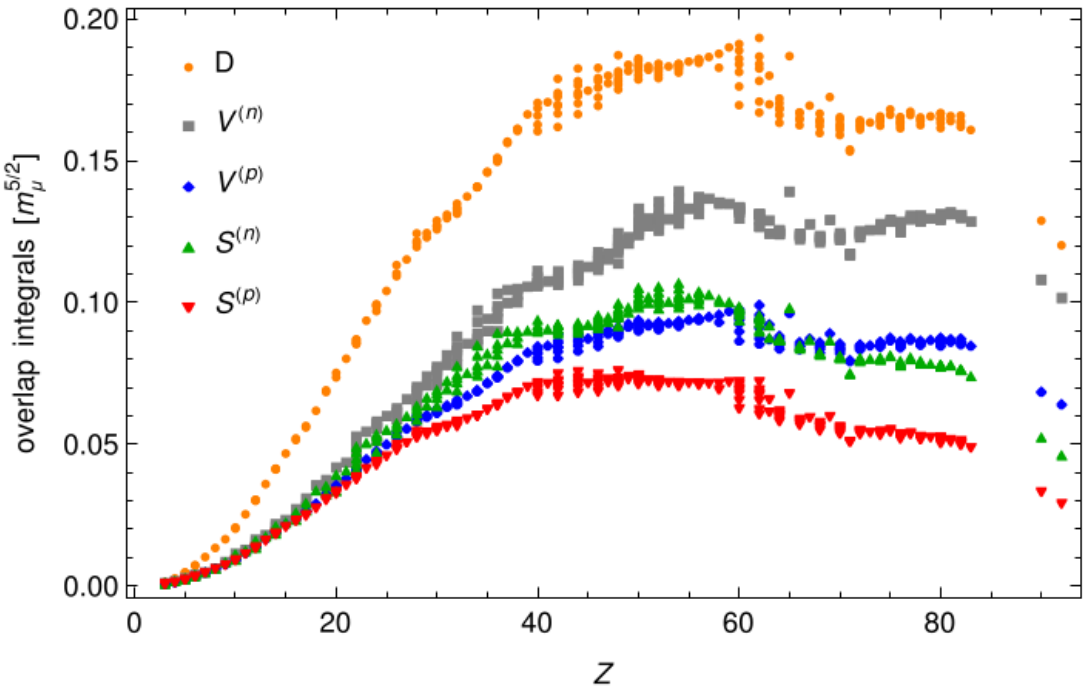

J. Heeck *et al.*, Nucl. Phys. B **980**, 115833 (2022)

- Overlap integral value decrease significantly at Z = 60 (Nd) due to quadrupole deformation

- Data come exclusively from electron scattering experiments
- For a number of isotopes, proton distribution computed only from rms radius
- Neutron distribution is equal to the proton distribution scaled by N/Z

Combining datasets using Barrett Moment

$$\langle r^k e^{-\alpha r} \rangle = \frac{4\pi}{Ze} \int \rho(r) r^k e^{-\alpha r} r^2 dr$$

Electron scattering experiment:

- map momentum transfer of electron to the Fourier transform of the charge distribution
- First term in the q^2 expansion corresponds to the rms radius $\langle r^2 \rangle = \int \rho(r) r^2 dr$

Muonic X-ray experiment:

- analysis of the hyperfine structure gives the charge distribution with its permanent quadrupole deformation
- for heavier nuclei, nuclear distributions with the same rms radius can generate different transition energies

$\Rightarrow$ Use Barrett moment instead of rms radius to enable the use of both electron scattering and muonic X-ray experimental data

R. Barrett, Phys. Lett. B **33**, 388 (1970)

Methodology

- Start with 3-parameter Fermi distribution (3pF)
  $\rho(r,\theta) = \frac{\rho_0}{1+\exp\left[\frac{r-c\left(1+\beta Y_{20}(\theta)\right)}{t}\right]}$

$\beta_{\lambda\mu} = 0$	$\beta_{20} > 0$	$\beta_{20} < 0$
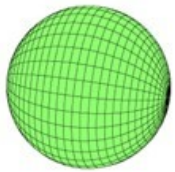	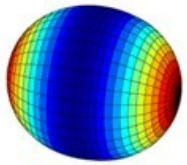	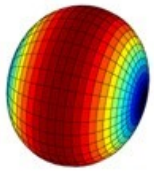

c: radius at half-density ; t: skin thickness ; β: quadrupole deformation parameter

- Convert it into a spherically-symmetric 2-parameter Fermi distribution ($\rho(r) = \frac{\rho_0}{1+\exp\left[\frac{r-c}{t}\right]}$) by adjusting the t parameter to keep a constant Barrett moment
- Solve the Dirac equation

Adding neutron distribution

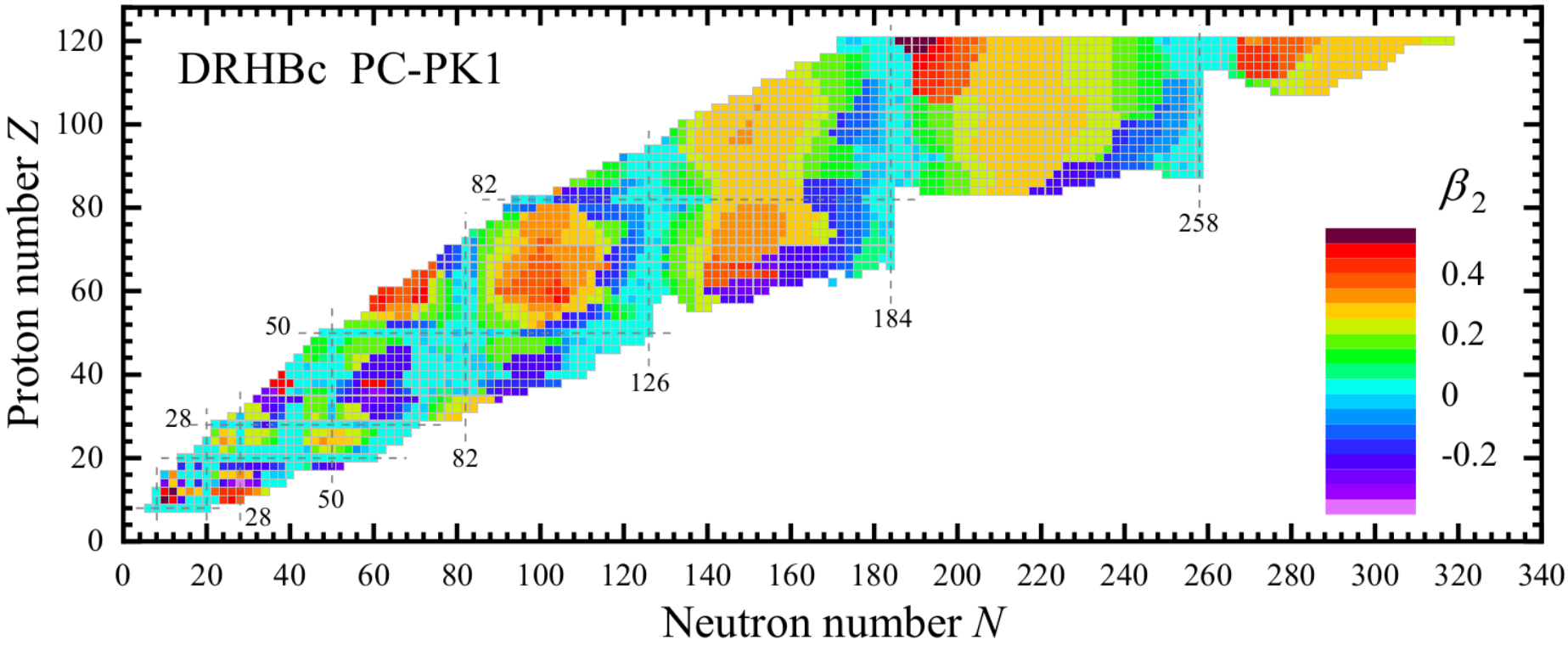

Calculation based on deformed relativistic Hartree-Bogoliubov model for even-even nuclei

K. Zhang *et al.*, At. Data Nucl. Data Tables **144**, 101488 (2022)

Results: all isotopes

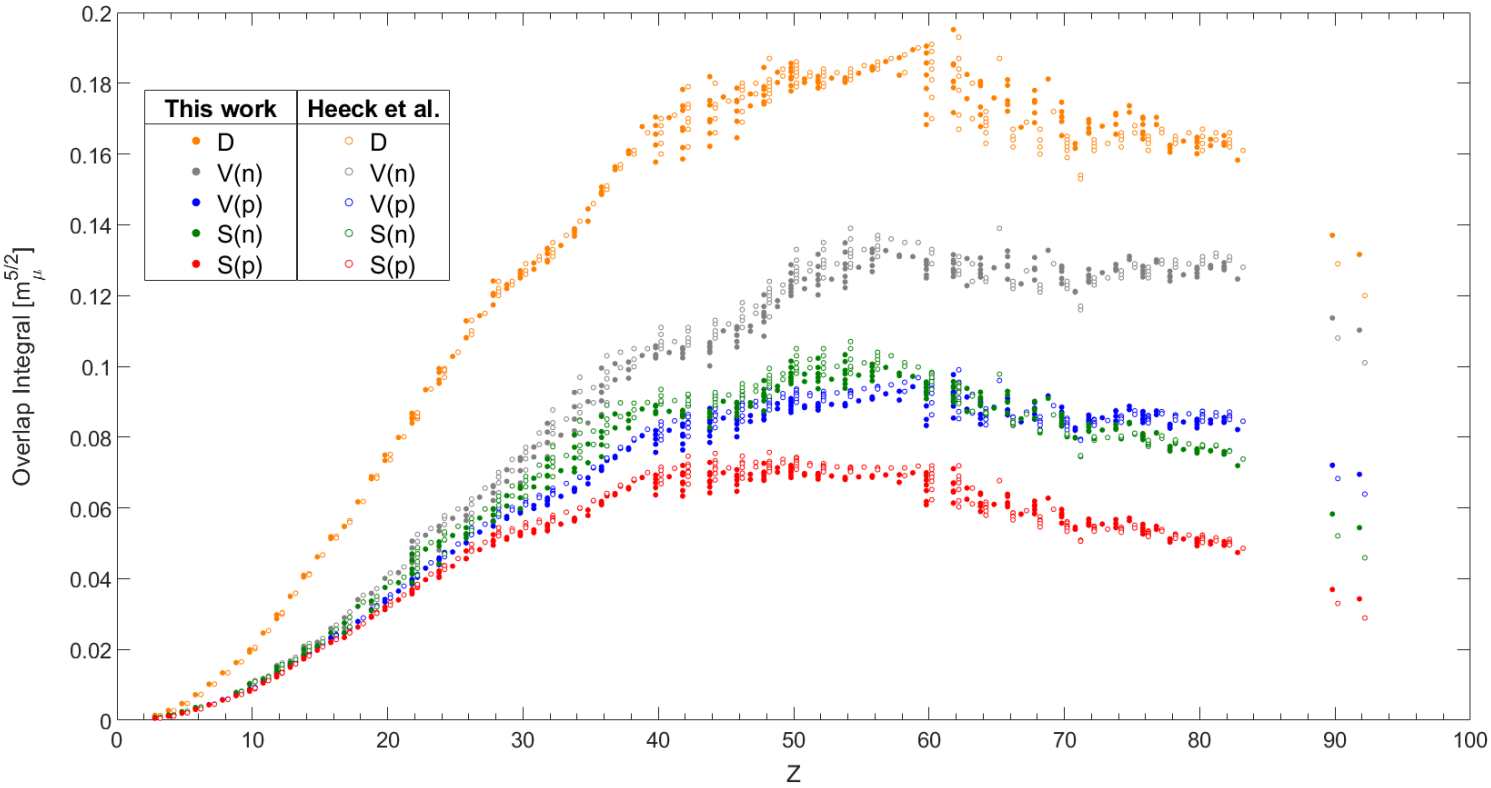

Overlap integral value in the deformed region (Z = 60-80) does not decrease as much

(datapoints from Heeck *et al.* shifted by +1/2 on the x-axis)

Results: natural abundance

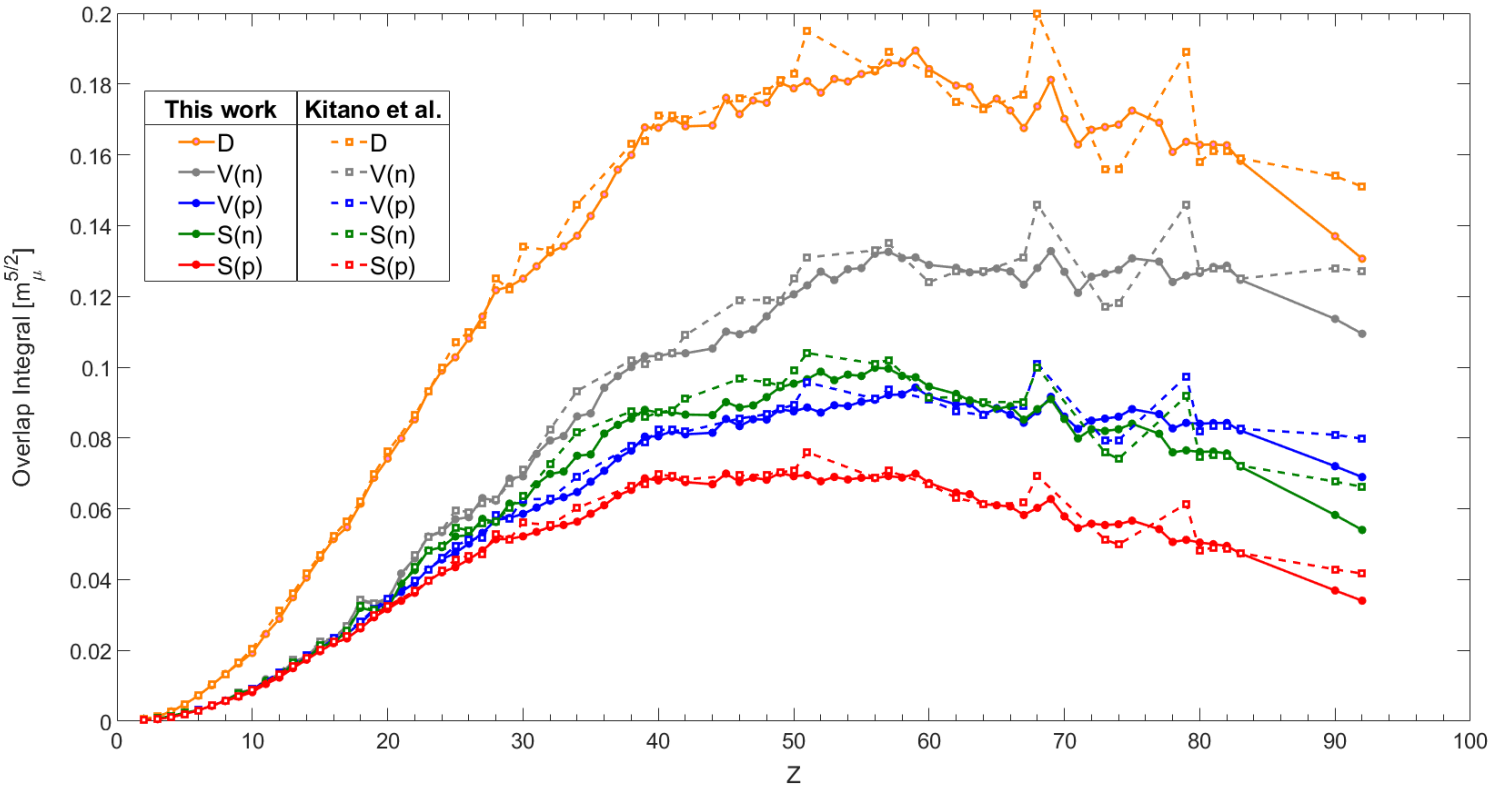

High variation in the data from Kitano *et al.* because they just pick one isotope (which may be highly deformed)

$\Rightarrow$ Natural abundance weighting softens variation

Experimental sensitivity plot (no normalization)

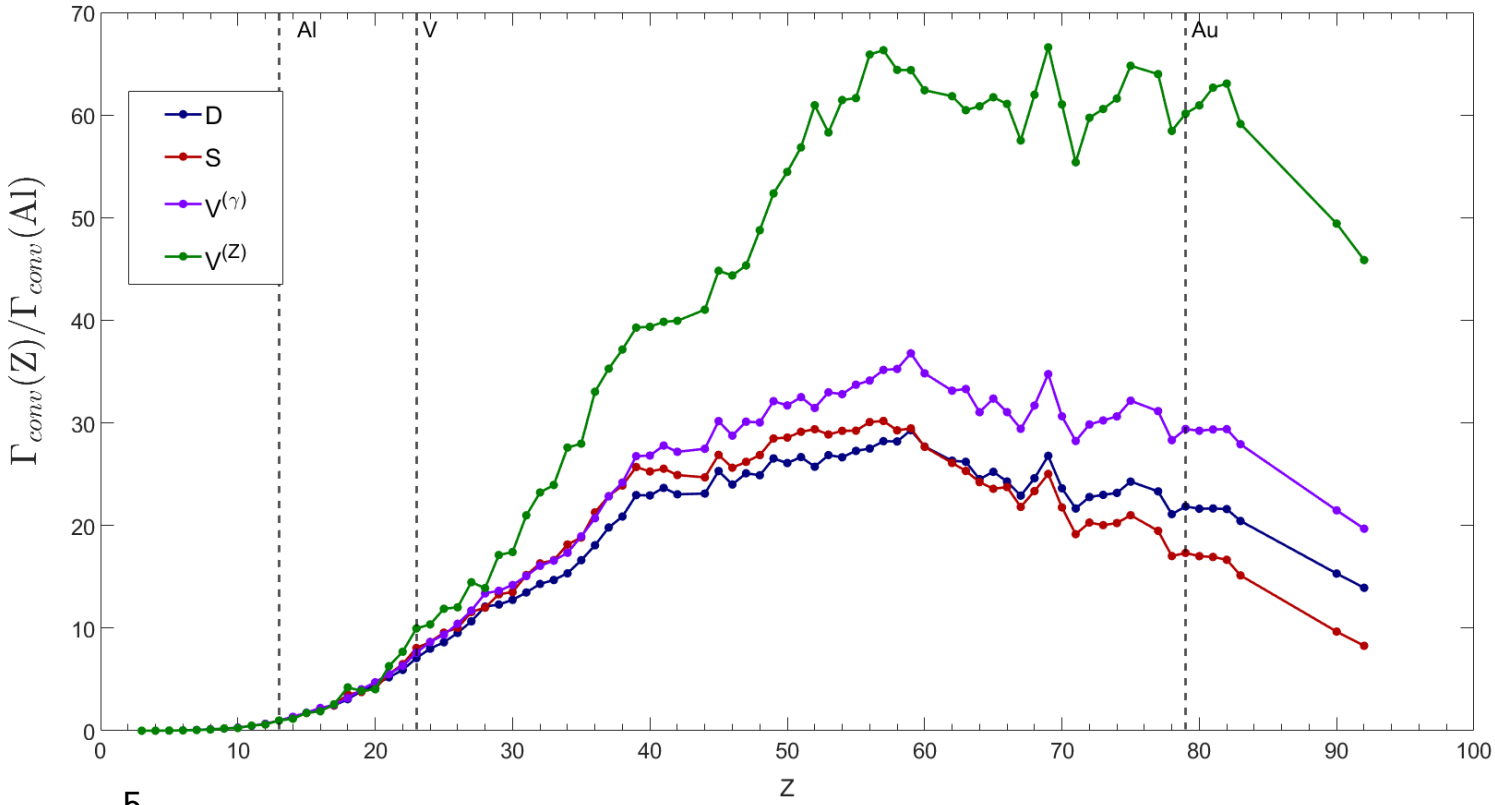

$$\Gamma^N_{\mu\to e} = \frac{m_\mu^5}{4\Lambda^4}\left|eC_L^D D_N + 4\left(G_F m_\mu m_p \tilde{C}^{SL}_{(p)} S_N^{(p)} + \tilde{C}^{VR}_{(p)} V_N^{(p)} + p \to n\right)\right|^2 + L \leftrightarrow R$$

This is the quantity measured directly by experiments!

A. Crivellin *et al.*, J. High Energy Phys. **5**, (2017)

Experimental sensitivity plot (muon capture rate)

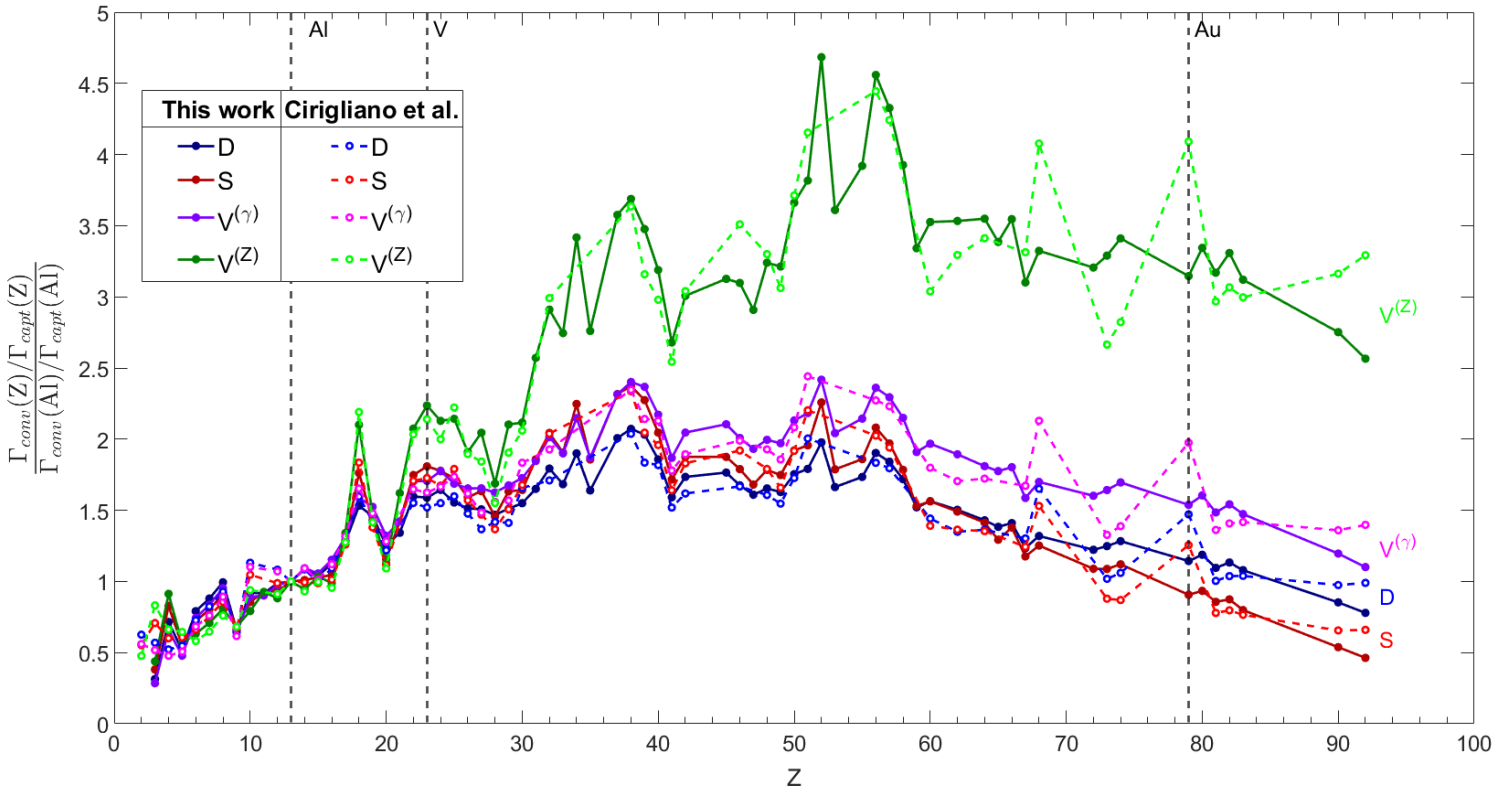

$$R_{\mu e}(A,Z) = \frac{\Gamma\left(\mu^- + N(A,Z) \to e^- + N(A,Z)\right)}{\Gamma(\mu^- + N(A,Z) \to \nu_\mu + N'(A,Z-1))} \sim \frac{\text{coherent process}}{\text{incoherent process}}$$

- Add in lots of variation due to nuclear effects

V. Cirigliano et al., Phys. Rev. D **80**, 013002 (2009)

Revision of historical CLFV experiments plot

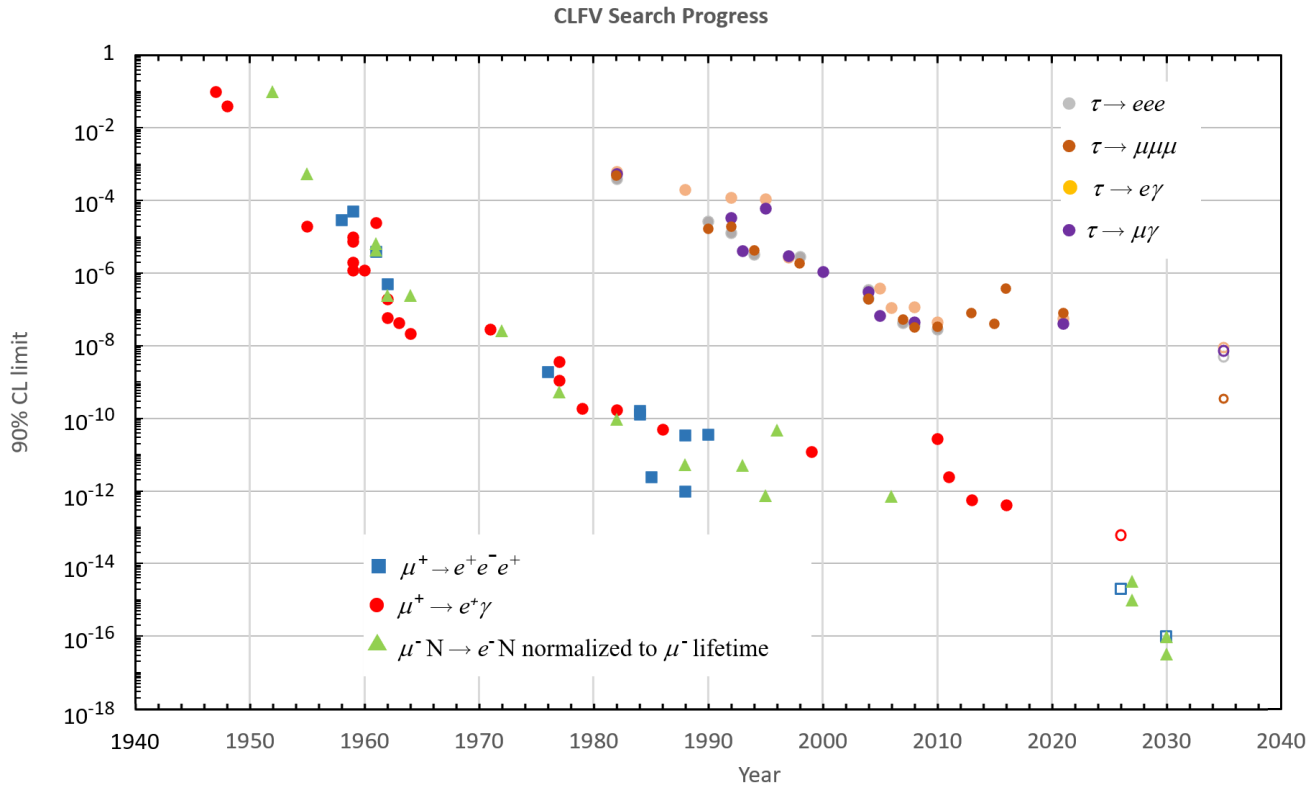

$$R_{\mu e}(A,Z) = \Gamma\left(\mu^- + N(A,Z) \to e^- + N(A,Z)\right) \cdot \tau_\mu$$

- $R_{\mu e}$ is not a true branching fraction, introduced by Weinberg and Feinberg (1959)
- Should use muon lifetime to compare with $\mu \to e\,\gamma$ experiments

Choice of target for future experiment

- Choose a target that complement Al search for the different type of contribution (dipole, scalar, or vector terms)
- Pseudo-scalar, axial, and tensor contribution only appears in spin-dependent conversion

Mu2e-II and AMF:

- ${}_{22}$Ti is a popular choice, but has multiple isotopes $\Rightarrow$ ${}_{23}$V has similar properties with only 1 main isotope
- Gold cannot be used for Mu2e-II because of pion-induced background ($\tau_{\mu}^{\mathrm{Au}} = 73ns$)
  - The Avanced Muon Facility (AMF) would solve this using a fixed-field alternating gradient synchrotron (FFA)

Conclusion

Improved the calculation of the coherent muon to electron conversion rate for a wide range of isotopes

1. Add muonic X-ray experimental data to electron scattering dataset
2. Include the effect of nuclear quadrupole deformation
3. Account for the difference between neutron and proton distribution
4. Present an alternative normalization for the muon conversion rate

Paper on the arXiv (2401.15025), under submisson to journal

Dirac Equation Solution

Radial solution of the Dirac equation:

$$\psi_\kappa^\mu = \begin{pmatrix} g(r)\,\chi_\kappa^\mu(\theta,\phi) \\ \mathrm{i}\,f(r)\,\chi_\kappa^\mu(\theta,\phi) \end{pmatrix}$$

Quantum numbers μ and κ:

$$(\sigma \cdot I + 1)\chi_\kappa^\mu = -\kappa\chi_\kappa^\mu \ , \ j_z\chi_\kappa^\mu = \mu\chi_\kappa^\mu$$

Dirac equation of the radial component (where $u_1(r) = r \cdot g(r)$ and $u_2(r) = r \cdot f(r)$):

$$\frac{d}{dr}\begin{pmatrix} u_1 \\ u_2 \end{pmatrix} = \begin{pmatrix} -\kappa/r & W - V + m_i \\ -(W - V - m_i) & \kappa/r \end{pmatrix}\begin{pmatrix} u_1 \\ u_2 \end{pmatrix}$$

Wavefunctions (for ^{27}Al nucleus)

- $1\,\mathrm{m}_\mu^{-1} \approx 1.868\,fm$
- Not exactly a free electron wavefunction: effect of the Al nucleus

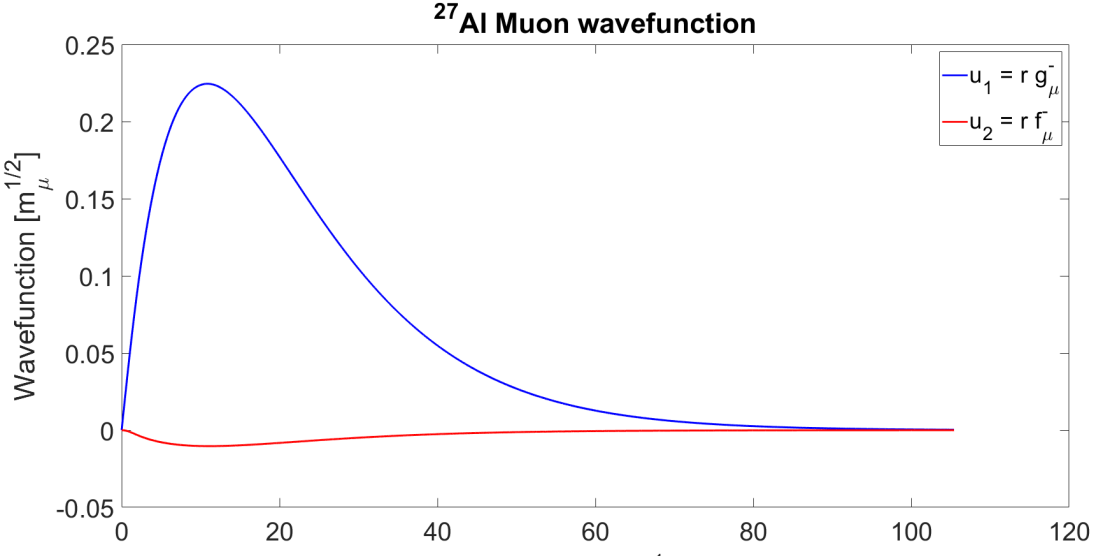

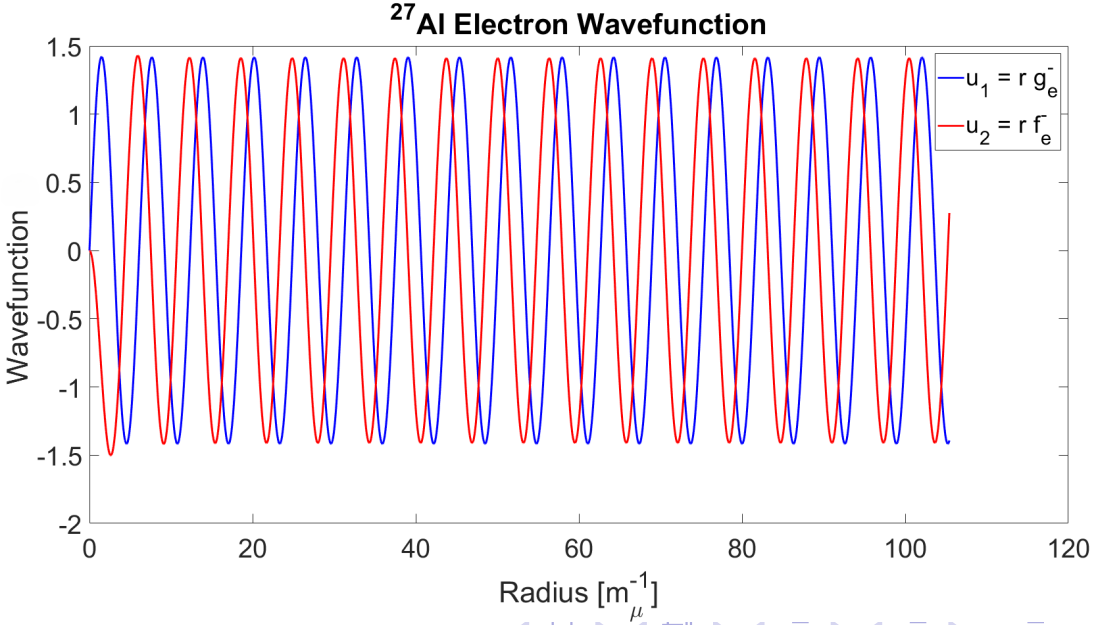

Barrett Moment parameter

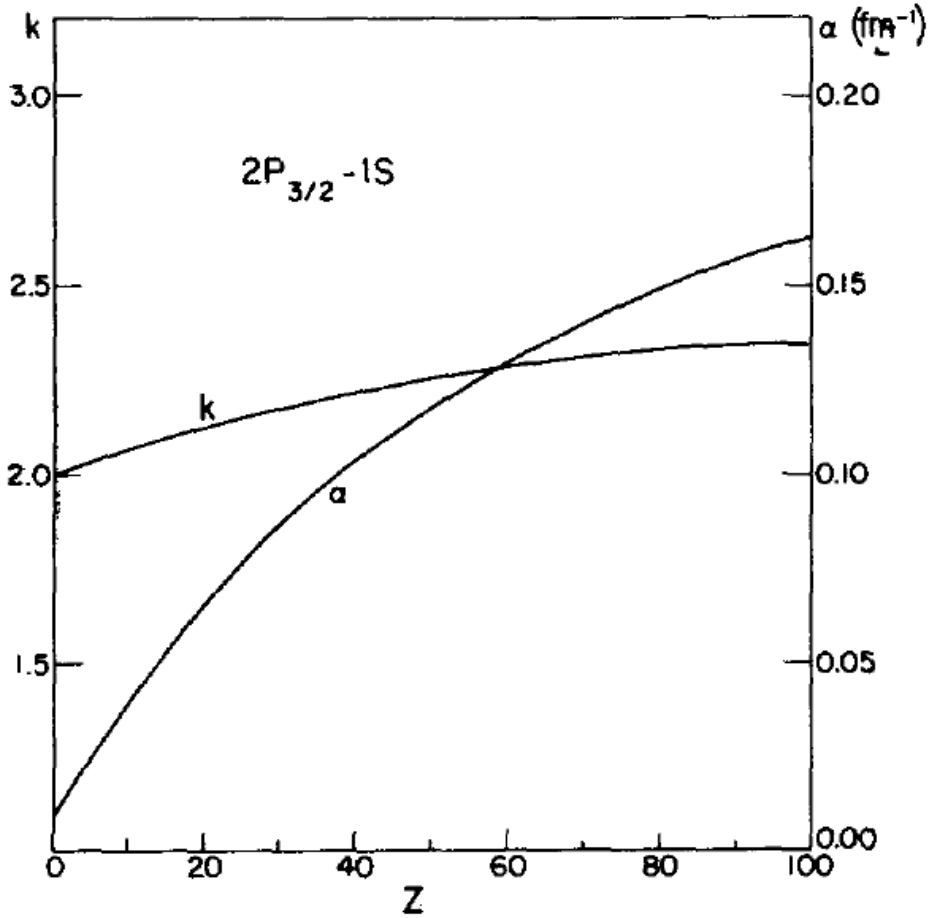

R. Barrett, Phys. Lett. B **33**, 388 (1970)

Case study: Isotopes of $_{60}$Nd

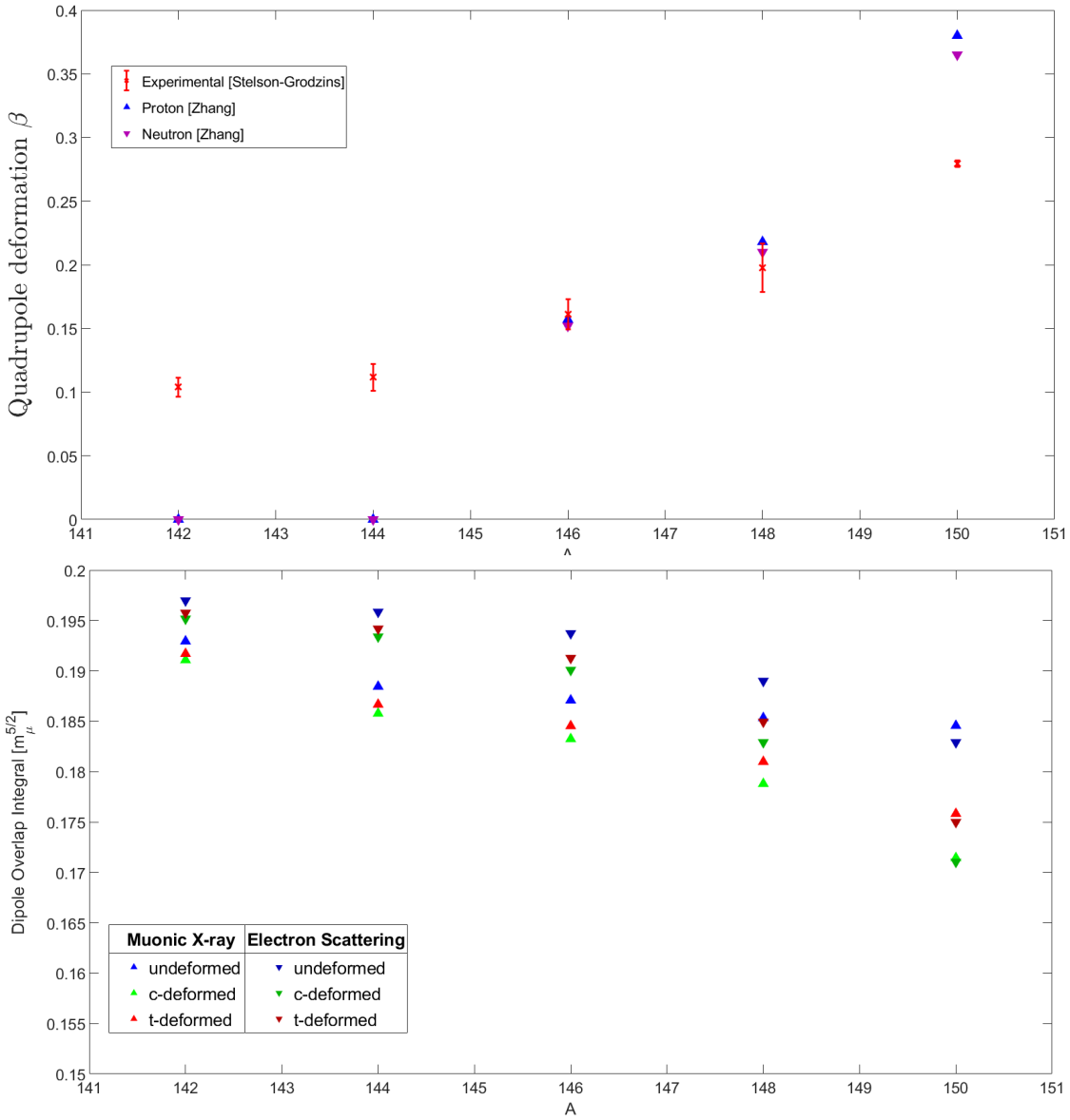

$_{60}$Nd is a great case study because its isotopes exhibit larger deformation as N increases

- Study the difference between electron scattering and muonic X-ray experimental datasets
- Study the impact of deforming using c or t
- Study the impact of using different distribution for proton and neutron

Uncertainties

Comparison of muonic X-ray and electron scattering determinations of 3pF in Nd

Isotope	c (fm)	t (fm)	β	*rms* radius (fm)	Barrett Moment
	Muonic X-ray				
^{142}Nd	5.80 ± 0.03	2.32 ± 0.08	0.104 ± 0.02	4.91 ± 0.08	15.99 ± 0.03
^{144}Nd	5.85 ± 0.03	2.27 ± 0.08	0.123 ± 0.02	4.94 ± 0.08	16.11 ± 0.04
^{146}Nd	5.82 ± 0.03	2.42 ± 0.08	0.151 ± 0.02	4.98 ± 0.08	16.26 ± 0.06
^{148}Nd	5.84 ± 0.03	2.40 ± 0.08	0.197 ± 0.04	5.00 ± 0.08	16.38 ± 0.13
^{150}Nd	5.86 ± 0.03	2.35 ± 0.08	0.279 ± 0.005	5.05 ± 0.08	16.58 ± 0.01
	Electron Scattering				
^{142}Nd	5.7045 ± 0.03	2.539 ± 0.013	0.104 ± 0.02	4.92 ± 0.08	15.98 ± 0.03
^{144}Nd	5.6634 ± 0.03	2.696 ± 0.013	0.123 ± 0.02	4.96 ± 0.08	16.11 ± 0.04
^{146}Nd	5.6600 ± 0.03	2.760 ± 0.013	0.151 ± 0.02	4.99 ± 0.08	16.23 ± 0.06
^{148}Nd	5.6871 ± 0.03	2.798 ± 0.022	0.197 ± 0.04	5.04 ± 0.08	16.46 ± 0.13
^{150}Nd	5.7185 ± 0.03	2.861 ± 0.031	0.279 ± 0.005	5.13 ± 0.08	16.86 ± 0.01

Historical CLFV experiments values

Atomic number-dependent adjustment of $\mu \rightarrow e$ conversion limits to normalization to muon stops rather than captures

Year	Experiment	Nucleus	90% CL Limit Normalized to μ Capture	90% CL Limit Normalized to μ Stops
1952	A. Lagarrigue *et al.*	Sn, Sb	1.0×10^{-1}	1.0×10^{-1}
1955	J. Steinberger *et al.*	Cu	5.0×10^{-4}	5.4×10^{-4}
1961	D. Sard *et al.*	Cu	4.0×10^{-6}	4.3×10^{-6}
1961	M. Conversi *et al.*	Cu	5.9×10^{-6}	6.4×10^{-6}
1962	G. Conforto *et al.*	Cu	2.2×10^{-7}	2.4×10^{-7}
1964	J. Bartley *et al.*	Cu	2.2×10^{-7}	2.4×10^{-7}
1972	D. Bryman *et al.*	Cu	2.6×10^{-8}	2.8×10^{-8}
1977	A. Badertscher *et al.*	S	4.0×10^{-10}	5.3×10^{-10}
1982	A. Badertscher *et al.*	S	7.0×10^{-11}	9.3×10^{-11}
1988	S. Ahmad *et al.*	Ti	4.6×10^{-12}	5.4×10^{-12}
1993	SINDRUM-II	Ti	4.3×10^{-12}	5.0×10^{-12}
1995	S. Eggli	Ti	6.5×10^{-13}	7.6×10^{-13}
1996	SINDRUM-II	Pb	4.6×10^{-11}	4.7×10^{-11}
2006	SINDRUM-II	Au	7.0×10^{-13}	7.2×10^{-13}